Clinical Trial/Experimental Study

Medicine®

OPEN

Integrated assessment of differentially expressed plasma microRNAs in subtypes of nonsyndromic orofacial clefts

Ni Wu, BS, Jun Yan, MS, Tao Han, MS, Jijun Zou, PhD*, Weimin Shen, PhD*

Abstract

Background: Orofacial clefts include cleft lip only (CLO), cleft palate only (CPO), and cleft lip with palate (CLP). Previously, we reported the expression profile of plasma microRNAs in CLO, CPO, and CLP, respectively. However, the interaction of each subtype remains poorly investigated.

Methods: In this study, we integrated the expression profiles of plasma miRNAs in these 3 subtypes, and assessed the distinct and overlapping dysregulated miRNAs using Venn diagrams. Their respective target genes reported in the literature were further analyzed using pathway analysis.

Results and conclusion: The results showed that distinct or overlapping signaling pathways were involved in CLO, CPO, and CLP. The common key gene targets reflected functional relationships to the Wnt, Notch, TGF-beta, and Hedgehog signaling pathways. Further studies should examine the mechanism of the potential target genes, which may provide new avenues for future clinical prevention and therapy.

Abbreviations: CLO = cleft lip only, CLP = cleft lip with palate, CPO = cleft palate only, KEGG = Kyoto Encyclopedia of Genes and Genomes, miRNAs = microRNAs, OFCs = orofacial clefts, qRT-PCR = real-time quantitative PCR, SBC = ShanghaiBio Corporation.

Keywords: cleft lip with palate, cleft palate, miRNA microarray, nonsyndromic cleft lip, plasma microRNA

1. Introduction

As common, complex birth defects with an overall birth prevalence of 1:800 live births worldwide,[1] orofacial clefts (OFCs) are categorized as cleft lip only (CLO) as usual, cleft palate only (CPO), and cleft lip with palate (CLP). The overall prevalence of OFCs in China was 1.4 per 1000 live births.[2] Around 70% of the whole of clefts were categorized as nonsyndromic, with no identifiable structural imperfection except for the clefts.[3] Children born with OFCs may encounter many difficulties in adapting to future social life, including feeding, language communication, dental development, hearing, and so on. Those influenced families will face tremendous financial burden and psychological distress from the community. The genetic causes of nonsyndromic clefts have been clarified gradually with the development of various ways including linkage, association studies, GWAS, exome sequencing, copy number variation, and whole-genome sequencing.[3–6] In addition, epigenetic data are able to assist in recognizing risk elements for OFCs or causal effects of clefts by disclosing epigenetic mechanisms, or by catching information about causal genetic or environmental points.[7,8]

As epigenetic factors, plasma miRNAs have emerged as attractive diagnostic and prognostic biomarkers for cancer, diabetes, allergic asthma, and oral cancers.[9–12] The identification of the plasma miRNA and potential targets' gene ontology and KEGG pathway enrichment is important to understand the regulatory mechanisms of CLO,[13] CPO, and CLP.[14] However, the interaction of each subtype remains poorly investigated. Recently, mounting evidence suggests there may be unique underlying pathophysiology and/or genetic modifiers influencing expression of these 3 subtypes of OFCs including CLO, CPO, and CLP.[7,15,16] Therefore, we explored whether children with different cleft subtypes showed distinct plasma miRNAs' profiles. In this study, we analyzed the expression profiles of plasma microRNAs in nonsyndromic CLO, CPO, and CLP as a whole using our previously reported human miRNA microarray data.[13,14] Based on KEGG pathway analysis, we found that there were distinct biological processes involving in the physiology of CLO, CPO, and CLP.

2. Materials and methods

2.1. Sample collection

Institutional Review Board of Nanjing Medical University (2014-10-16) has approved this research. Nonsyndromic cleft lip (CLO), cleft palate (CPO), and cleft lip with palate (CLP) patients' plasma samples were collected using methods as we

Editor: Fabricio Ferreira de Oliveira.

NW and JY contributed equally to this work.

This study was supported by the Science and Technology Development Foundation of Nanjing Medical University (2016NJMUZD058).

The authors have no conflicts of interest to disclose.

Supplemental Digital Content is available for this article.

Department of Burns and Plastic Surgery, Children's Hospital of Nanjing Medical University, Gulou Area, Nanjing, Jiangsu, China.

* Correspondence: Weimin Shen, Department of Burns and Plastic Surgery, Children's Hospital of Nanjing Medical University, No. 72 Guangzhou Road, Gulou Area, Nanjing, Jiangsu 210008, China. Business (e-mail: swmswmswm@sina.com; drshenweimin@163.com), Jijun Zou (e-mail: 5098782@qq.com).

Medicine (2018) 97:25(e11224)

Received: 21 December 2017 / Accepted: 1 June 2018

http://dx.doi.org/10.1097/MD.0000000000011224

previously described.[13,14] EDTAK2 tubes (regular type) were utilized to collect the peripheral blood. The supernatant plasma was centrifuged at 12,000 g for 10 minutes. The supernatant was aliquoted and stored at −80°C.

2.2. Human miRNA microarray analysis

Twelve plasma samples were divided into 4 groups including CLO (n = 3), CPO (n = 3), CLP (n = 3), and control (n = 3). These 4 groups were analyzed using human miRNA microarray chips (8×60K) v21.0 as we previously described.[13,14] miRNAs that show expression changes above twofold were selected. We draw Venn diagrams on this website (http://bioinformatics.psb.ugent.be/webtools/Venn/).

2.3. KEGG pathway enrichment analyses

We use miRTarbase and Tarbase databases through the ShanghaiBio Corporation (SBC) online (http://sas.ebioservice.com) to predict the target genes of these differentially expressed plasma miRNAs. KEGG pathway enrichment analyses were performed as we previously described.[13] Fisher's exact test was utilized to conduct the calculation of the enrichment *P*-values of the pathway enrichment analyses, which was rectified applying enrichment *q*-values (the false discovery rate) that were computed utilizing the method of John Storey.

3. Results

3.1. miRNA microarray and bioinformatics analysis

The 4 groups CLO, CPO, CLP, and control of plasma miRNA microarray analysis were displayed using hierarchical clustering (Fig. 1A). Scatter plot visualization showed miRNAs expression variation between the 2 groups of control and CLO, control and CPO, control and CLP, CLO, and CPO, CLO, and CLP, CPO and CLP (Fig. 1B). Red dots represent a twofold or greater upregulation between the 2 groups, green dots refer to a twofold or greater downregulation between the 2 groups (Fig. 1B). Upregulated or downregulated miRNAs' numbers were shown in Figure 1B. Correlation analysis of these expressed miRNAs in the control, CLO, CPO, and CLP plasma samples revealed that CLO was closely related to CLP (Fig. 1C). The correlation coefficient between CLO and CLP was 0.9749, meaning that CLO was highly correlated with CLP.

We selected differentially expressed plasma miRNAs that showed expression changes above twofold (compared to the control group) in the CLO, CPO, and CLP groups. Overlapping data sets were performed using Venn diagrams (Fig. 1D). Totally, 57 miRNAs were co-upregulated among the CLO, CPO, and CLP plasma samples (Fig. 1D). Table 1 shows all those co-upregulated miRNAs (fold change≥2). Among these CLO, CPO, and CLP plasma samples, 45 miRNAs were co-downregulated (Fig. 1D). Table 2 shows all these co-downregulated miRNAs (fold change≥2).

Previously, we have demonstrated the expression changes of several miRNAs in larger samples of CLO, CPO, and CLP using BulgeLoop qRT-PCR, and confirmed that the miRNA microarray data was confidential.[13,14] Therefore, we performed bioinformatics analysis as follows using these differentially expressed miRNAs in respective groups.

3.2. Functional analysis of potential target genes of co-expressed dysregulated miRNAs

We want to examine whether there are overlapping biological processes involved among CLO, CPO, and CLP groups.

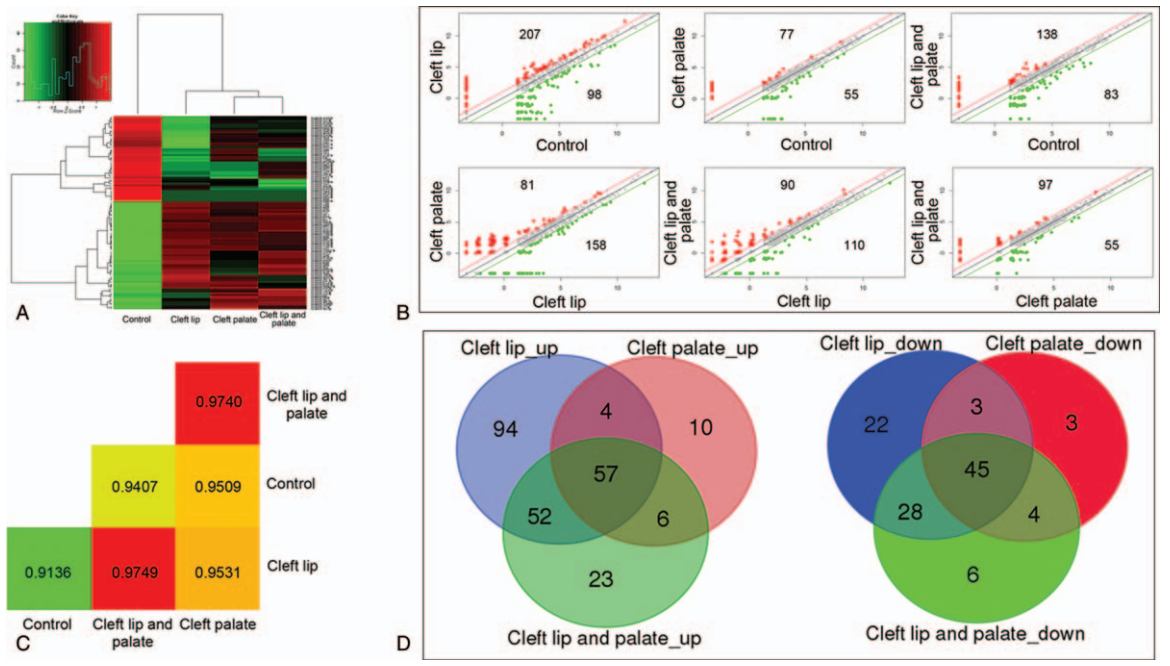

Figure 1. Plasma miRNA microarray expression data among the patients with nonsyndromic CLO, CPO, CLP, and healthy children. (A) Hierarchical clustering reveals the miRNA expression profile. (B) Scatter plot represents the differentially expressed miRNAs between indicated groups. The miRNAs numbers are listed above the data dot. (C) Correlation analysis shows the relationship between indicated groups. (D) Venn diagrams show the number of distinct and overlapping upregulated or downregulated miRNAs among CLO, CPO, and CLP. CLO = cleft lip only, CLP = cleft lip with palate, CPO = cleft palate only, miRNAs = microRNAs.

Table 1

List of 57 miRNAs that were co-overexpressed in CLO, CPO, and CLP plasma samples.

miRNA	Fold change in CLO	Fold change in CPO	Fold change in CLP	Mirbase_accession_no
hsa-let-7f-5p	4.411882504	36.22596962	94.70817	MIMAT0000067
hsa-miR-1182	30.90972899	21.12385297	26.03614	MIMAT0005827
hsa-miR-1185-2-3p	43.70022189	35.1702528	22.02562	MIMAT0022713
hsa-miR-1226-5p	41.43600474	33.54898467	41.68948	MIMAT0005576
hsa-miR-1249-3p	40.2654988	40.65460578	26.77842	MIMAT0005901
hsa-miR-139-3p	9.51518129	9.764356234	30.04384	MIMAT0004552
hsa-miR-144-5p	3.663147516	22.12870316	34.8168	MIMAT0004600
hsa-miR-150-5p	6.298554621	2.004063192	5.130724	MIMAT0000451
hsa-miR-17-3p	9.220642001	25.74651928	10.66161	MIMAT0000071
hsa-miR-195-5p	4.448338761	11.29175573	10.05747	MIMAT0000461
hsa-miR-215-5p	24.41000863	10.32330917	24.41001	MIMAT0000272
hsa-miR-27b-3p	21.6131448	10.79146345	4.974262	MIMAT0000419
hsa-miR-30b-5p	24.63448831	43.52249926	53.10868	MIMAT0000420
hsa-miR-30c-1-3p	23.91295476	9.047680623	4.742653	MIMAT0004674
hsa-miR-30c-5p	4.124204869	10.41075678	4.763296	MIMAT0000244
hsa-miR-3156-5p	47.15106983	39.43275489	33.64425	MIMAT0015030
hsa-miR-3158-5p	50.8968124	36.59335278	29.4613	MIMAT0019211
hsa-miR-3648	7.345623232	2.844126433	7.529149	MIMAT0018068
hsa-miR-374a-5p	10.93947221	41.43600474	53.56016	MIMAT0000727
hsa-miR-3945	91.10153136	54.65085267	55.2666	MIMAT0018361
hsa-miR-424-5p	29.2495414	11.54279821	23.91295	MIMAT0001341
hsa-miR-4314	84.61940287	48.61549818	91.10153	MIMAT0016868
hsa-miR-4417	43.88762515	39.91649111	27.81709	MIMAT0018929
hsa-miR-4496	36.59335278	21.48931067	25.86879	MIMAT0019031
hsa-miR-4508	32.39944736	20.71298968	22.6453	MIMAT0019045
hsa-miR-4673	9.853576931	23.30205038	21.36562	MIMAT0019755
hsa-miR-4688	22.12870316	9.853576931	37.87732	MIMAT0019777
hsa-miR-4698	2.733719842	2.111650978	2.899994	MIMAT0019793
hsa-miR-4707-3p	62.15609659	53.56016129	88.45938	MIMAT0019808
hsa-miR-4716-3p	37.70468783	25.26925455	22.1287	MIMAT0019827
hsa-miR-4734	24.85582183	10.0100476	24.63449	MIMAT0019859
hsa-miR-4769-5p	28.7644843	10.6616052	4.959765	MIMAT0019922
hsa-miR-532-5p	9.074101253	10.62257173	4.541014	MIMAT0002888
hsa-miR-550a-3-5p	25.74651928	22.36834171	10.8752	MIMAT0020925
hsa-miR-564	26.77841749	9.835220996	47.83535	MIMAT0003228
hsa-miR-601	34.81679985	35.01135033	36.03937	MIMAT0003269
hsa-miR-6071	39.91649111	21.23769516	52.38286	MIMAT0023696
hsa-miR-6133	44.47107271	10.44385581	27.50138	MIMAT0024617
hsa-miR-660-5p	21.36561589	24.63448831	28.21952	MIMAT0003338
hsa-miR-663a	68.82300594	28.7644843	47.35553	MIMAT0003326
hsa-miR-6738-5p	41.6894808	9.491392176	40.3395	MIMAT0027377
hsa-miR-6748-5p	21.71603486	10.37443433	20.60795	MIMAT0027396
hsa-miR-6758-5p	23.68297967	23.39995743	9.81465	MIMAT0027416
hsa-miR-6774-5p	25.26925455	20.60794724	4.699301	MIMAT0027448
hsa-miR-6777-3p	47.83535169	35.46737616	53.8186	MIMAT0027455
hsa-miR-6784-5p	52.70695713	33.23554485	28.4822	MIMAT0027468
hsa-miR-6807-5p	33.54898467	27.50138174	34.4576	MIMAT0027514
hsa-miR-6820-5p	25.86879055	22.91788016	39.11779	MIMAT0027540
hsa-miR-6887-5p	28.39722992	28.48219643	22.30914	MIMAT0027674
hsa-miR-6889-5p	39.11779377	9.571469583	39.91649	MIMAT0027678
hsa-miR-7109-5p	28.48219643	22.30913853	20.89674	MIMAT0028115
hsa-miR-711	44.62965658	21.6131448	28.39723	MIMAT0012734
hsa-miR-7114-5p	4.751631743	9.411870237	23.30205	MIMAT0028125
hsa-miR-8060	31.29330435	29.71087523	24.85582	MIMAT0030987
hsa-miR-8089	33.23554485	9.716781315	22.36834	MIMAT0031016
hsa-miR-877-5p	42.23652977	36.42551336	38.19915	MIMAT0004949
hsa-miR-96-5p	4.222786477	43.70022189	30.35895	MIMAT0000095

CLO = cleft lip only, CLP = cleft lip with palate, CPO = cleft palate only, miRNAs = microRNAs.

Therefore, we performed KEGG pathway analysis. Around 57 co-upregulated and 45 co-downregulated miRNAs among CLO, CPO, and CLP groups could produce 13,846 nonduplicated target genes reported in the literature using the miRTarbase and Tarbase (Supplemental file 1, http://links.lww.com/MD/C302). The top 30 enriched pathways for these 13,846 nonduplicated target genes are listed in Figure 2. Overall, these 13,846 target genes were involved in

Table 2

List of 45 miRNAs that were co-downregulated in CLO, CPO, and CLP plasma samples.

miRNA	Fold change in CLO	Fold change in CPO	Fold change in CLP	Mirbase_accession_no
hsa-miR-1237-3p	0.076495	0.0428	0.178651	MIMAT0005592
hsa-miR-1260a	0.121937	0.421973	0.188688	MIMAT0005911
hsa-miR-1281	0.01084	0.292046	0.361803	MIMAT0005939
hsa-miR-1304-3p	0.020689	0.022516	0.021418	MIMAT0022720
hsa-miR-1825	0.018396	0.305342	0.315741	MIMAT0006765
hsa-miR-191-3p	0.042235	0.210028	0.202306	MIMAT0001618
hsa-miR-193a-5p	0.42512	0.42512	0.1725	MIMAT0004614
hsa-miR-221-3p	0.14276	0.385379	0.317683	MIMAT0000278
hsa-miR-3187-3p	0.012759	0.013886	0.013209	MIMAT0015069
hsa-miR-338-3p	0.084885	0.0428	0.214453	MIMAT0000763
hsa-miR-4286	0.173823	0.481617	0.148742	MIMAT0016916
hsa-miR-4290	0.039327	0.0428	0.040714	MIMAT0016921
hsa-miR-4428	0.346344	0.354171	0.170319	MIMAT0018943
hsa-miR-4433a-5p	0.034343	0.207867	0.084119	MIMAT0020956
hsa-miR-4455	0.024617	0.422613	0.365739	MIMAT0018977
hsa-miR-4649-3p	0.018164	0.200187	0.091757	MIMAT0019712
hsa-miR-4668-5p	0.033727	0.389545	0.170031	MIMAT0019745
hsa-miR-4728-5p	0.188386	0.471993	0.412945	MIMAT0019849
hsa-miR-4738-3p	0.165863	0.356057	0.151948	MIMAT0019867
hsa-miR-4749-3p	0.210457	0.431131	0.458677	MIMAT0019886
hsa-miR-4769-3p	0.02459	0.2995	0.328468	MIMAT0019923
hsa-miR-494-3p	0.469749	0.421072	0.074374	MIMAT0002816
hsa-miR-574-5p	0.06771	0.398578	0.302998	MIMAT0004795
hsa-miR-636	0.086762	0.405199	0.173279	MIMAT0003306
hsa-miR-6508-5p	0.019746	0.02149	0.091996	MIMAT0025472
hsa-miR-6515-3p	0.108892	0.233031	0.255185	MIMAT0025487
hsa-miR-6732-3p	0.027103	0.029497	0.129832	MIMAT0027366
hsa-miR-6751-3p	0.007734	0.096354	0.272251	MIMAT0027403
hsa-miR-6776-5p	0.091188	0.023691	0.022536	MIMAT0027452
hsa-miR-6785-5p	0.393605	0.292436	0.215104	MIMAT0027470
hsa-miR-6797-3p	0.023712	0.486474	0.356753	MIMAT0027495
hsa-miR-6800-3p	0.080329	0.207097	0.209525	MIMAT0027501
hsa-miR-6813-3p	0.047833	0.2951	0.244702	MIMAT0027527
hsa-miR-6851-3p	0.0261	0.028405	0.109846	MIMAT0027603
hsa-miR-6861-3p	0.025484	0.027735	0.119237	MIMAT0027624
hsa-miR-6870-3p	0.039327	0.0428	0.040714	MIMAT0027641
hsa-miR-6873-3p	0.020278	0.022069	0.020993	MIMAT0027647
hsa-miR-6880-3p	0.039327	0.0428	0.040714	MIMAT0027661
hsa-miR-7111-3p	0.020534	0.022348	0.227218	MIMAT0028120
hsa-miR-7114-3p	0.039327	0.0428	0.180041	MIMAT0028126
hsa-miR-7641	0.411015	0.466679	0.29544	MIMAT0029782
hsa-miR-766-3p	0.124666	0.248389	0.280315	MIMAT0003888
hsa-miR-7975	0.121586	0.443054	0.153591	MIMAT0031178
hsa-miR-7977	0.159547	0.425408	0.15303	MIMAT0031180
hsa-miR-8073	0.197354	0.0428	0.462327	MIMAT0031000

CLO = cleft lip only, CLP = cleft lip with palate, CPO = cleft palate only, miRNAs = microRNAs.

Wnt, p53, TGF-beta, and Hedgehog signaling pathways (Fig. 3).

3.3. Function analysis of the potential target genes of the miRNAs dysregulated in CLO, CPO, or CLP, respectively

To explore whether distinct biological processes regulated CLO, CPO, and CLP, we performed KEGG pathway analysis of the forecasted targets of the distinctively expressed miRNAs in CLO, including 94 upregulated miRNAs and 22 downregulated miRNAs yielding 14,114 nonduplicated potential target genes (Supplemental file 2, http://links.lww.com/MD/C303). The top 30 enriched KEGG pathways for the 14,114 potential target genes of the dysregulated miRNAs in CLO showed that those genes were mainly involved in Wnt, Notch, TGF-beta, and Hedgehog signaling pathways (Fig. 4). Then, we performed KEGG analysis of the forecasted targets of the distinctively expressed miRNAs in CPO, including 10 upregulated miRNAs and 3 downregulated miRNAs producing 9330 nonduplicated possible target genes (Supplemental file 3, http://links.lww.com/MD/C304). The top 30 enriched KEGG pathways are listed in Figure 5. The analysis revealed that the potential target genes of the dysregulated miRNAs in CPO were associated with the Wnt, p53, Notch, and Hedgehog signaling pathways (Fig. 5). Additionally, we performed KEGG analysis of the forecasted targets of the distinctively expressed miRNAs in CLP, including

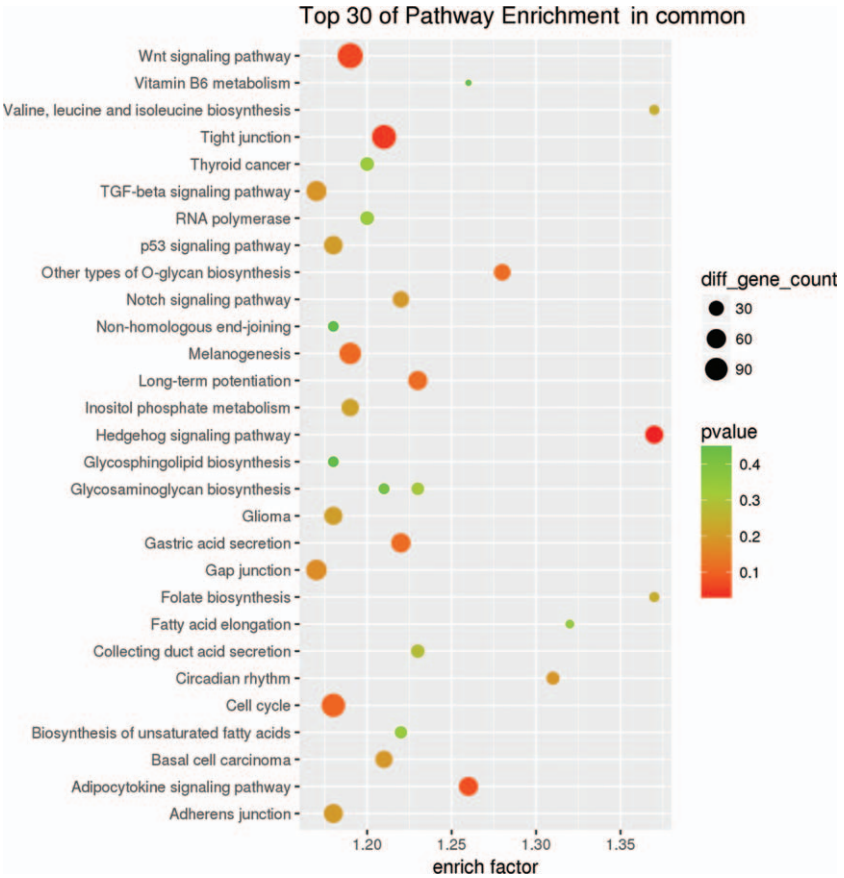

Figure 2. KEGG pathway analyses show the associated function of the target genes of the miRNAs dysregulated among CLO, CPO and CLP. Top 30 enriched pathways for the 13846 target genes of the 57 upregulated miRNAs and 45 downregulated miRNAs among the CLO, CPO and CLP. Fisher's exact test is utilized to calculate the enrichment *P*-value. Based on the first letter of the path name, the terms/paths on the vertical axis are sorted in descending order. Enrichment factors are plotted on the horizontal axis, that is, the number of dysregulated genes/total number of dysregulated genes in the pathway/(number of genes in the pathway in the database/total number of genes in the database). The first 30 enrichment approaches are based on enrichment factors. Pathway in the number of genes ≥ 4, $P < .05$ is the selection criteria. *P*-values are expressed in different colors from green to red. The different sizes of the round shapes represent the gene count number in a pathway. CLO = cleft lip only, CLP = cleft lip with palate, CPO = cleft palate only, KEGG = Kyoto Encyclopedia of Genes and Genomes, miRNAs = microRNAs.

23 upregulated miRNAs and 6 downregulated miRNAs creating 11,232 nonduplicated possible target genes (Supplemental file 4, http://links.lww.com/MD/C305). The top 30 enriched KEGG pathways revealed that the potential target genes of the dysregulated miRNAs in CLP were associated with the Wnt, TGF-beta, Notch, and Hedgehog signaling pathways (Fig. 2).

To clarify their relationship among CLO, CPO, and CLP, we illustrated the overlapping top 30 KEGG pathways among the 3 data sets using Venn diagrams (Fig. 6). As shown in Figure 6, 12 common KEGG pathways were enriched in the 3 CLO, CPO, and CLP groups, including Wnt, Notch, and Hedgehog signaling pathway (Fig. 6). Ten specific KEGG pathways were involved in CLO, including Valine, leucine, and adipocytokine signaling pathway (Fig. 6). Ten specific KEGG pathways were involved in CPO, including basal transcription factors, Lysine biosynthesis, and neurotrophin signaling pathway (Fig. 6). Whereas 10 specific KEGG pathways were involved in CLP, including regulation of autophagy, insulin signaling pathway, and mTOR signaling pathway (Fig. 6).

4. Discussion

To our knowledge, plasma miRNAs are highly stable.[17] Exploring the functions of plasma miRNAs in CLO, CPO, and CLP will help us to understand the physiology and development of these 3 diseases. In this study, we used microarray profiling to deeply assess the interactions and distinctions of plasma miRNAs among CLO, CPO, and CLP patients. A total of 207 miRNAs were upregulated and 98 miRNAs were downregulated in the CLO plasma samples compared to the control. 77 miRNAs were upregulated and 55 miRNAs were downregulated in the CPO plasma samples compared to the control. Around 138 miRNAs were upregulated and 83 miRNAs were downregulated in the CLP plasma samples compared to the control. Further elucidating these plasma miRNAs' roles in orofacial clefts would provide clues for preventing OFCs.

A lot of evidence has proved that the etiological mechanisms of CLP and CPO are distinct.[18,19] Some studies reveal that nonsyndromic orofacial clefts have identical configurations.[20,21] Recently, CPO was reported to have unrelated genetic factors and should be examined independently.[22,23] In our study, we found that CLO was highly correlated with CLP based on correlation analysis.

Venn diagrams were new method to visualize the complex genetic set relations.[24] Here, we found that 57 miRNAs were co-upregulated in CLO, CPO, and CLP plasma samples, whereas 45 miRNAs were co-downregulated in CLO, CPO, and CLP plasma samples.

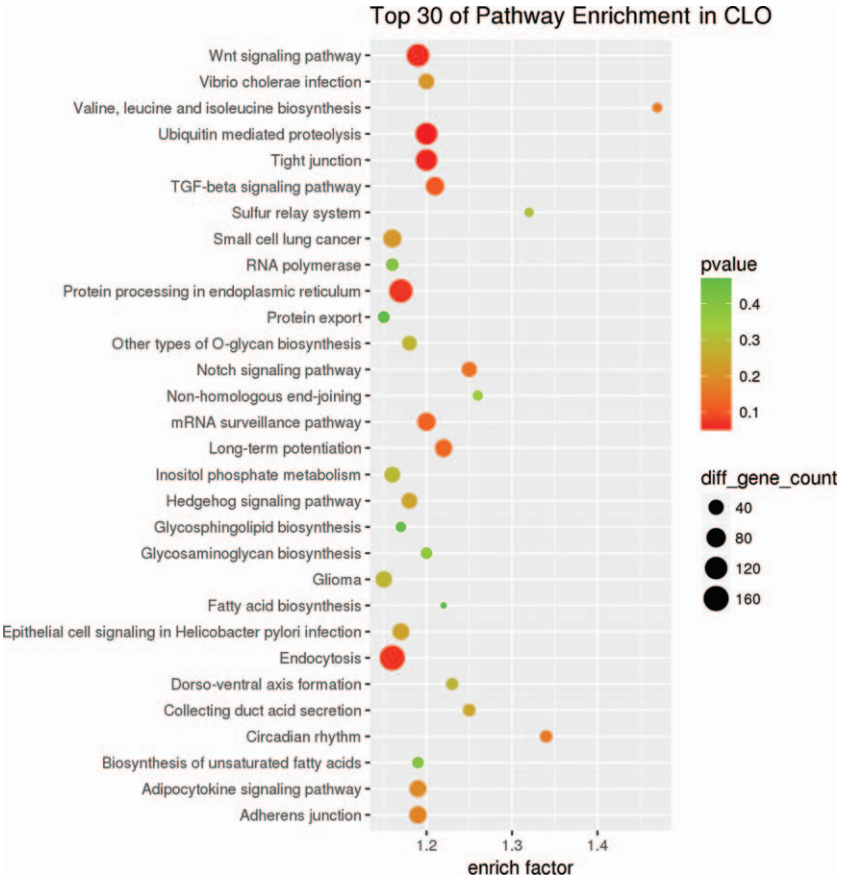

Figure 3. KEGG pathway analyses show the associated function of the target genes of the miRNAs dysregulated in CLO. The top 30 enriched pathways for the 14114 target genes of the 94 upregulated miRNAs and 22 downregulated miRNAs in CLO. The enrichment *P*-values were calculated using Fisher's exact test. The term/pathway on the vertical axis was drawn according to the first letter of the pathway name in descending order. The horizontal axis represents the enrichment factor, that is, (the number of dysregulated genes in a pathway/the total number of dysregulated genes)/(the number of genes in a pathway in the database/the total number of genes in the database). The top 30 enriched pathways were selected according to the enrichment factor value. The selection standards were the number of genes in a pathway ≥4 and $P < .05$. The different colours from green to red represent the *P*-value. The different sizes of the round shapes represent the gene count number in a pathway. CLO = cleft lip only, miRNAs = microRNAs, KEGG = Kyoto Encyclopedia of Genes and Genomes.

One limitation of our study was that we performed 4 miRNA microarray chips using 12 samples. Therefore, no *P*-values were got properly. Thus, these results in Tables 1 and 2 are reported in fold change values instead of *P*-values. The other limitation was that we used small samples (N = 3 for each group) for microarray chip assay. Whereas 6 selected plasma miRNAs including miR-16-2-3p, miR-215-5p, miR-365a-3p, miR-574-5p, miR-584-5p, and miR-877-5p were validated using qRT-PCR between another 13 CLO and 11 healthy children as we reported previously.[13] We also checked another 6 plasma miRNAs including miR-340-5p, miR-877-5p, miR-3648, miR-1260a, miR-494-3p, and miR-1304-3p among 16 CPO, 33 CLP, and 8 healthy children using qRT-PCR.[14] The results revealed that qRT-PCR verification data were consistent with the miRNAs microarray data.[13,14] Thus, our miRNAs microarray data are reliable and we could conduct bioinformatics analysis for key genes and pathways participated in CLO, CPO, and/or CLP pathogenesis based on the microarray data.

One of the crucial pathological reasons of orofacial clefts is unusual craniofacial development. MiRNAs played important roles in craniofacial development.[25–27] In addition, SNPs in the miRNA-binding sites or miRNA processing genes were announced to be linked to nonsyndromic orofacial clefts susceptibility.[28,29] In mammals, it is possible for miRNAs to control 30% of the protein-coding genes by means of posttranscriptional silencing; therefore, the dysregulation of miRNAs in CLO, and it is possible for CPO or CLP patients have a far-reaching impact on a wide range of roles in biology. Based on our miRNA microarray data, we found the intersection of differentially expressed miRNAs in CLO, CPO, and CLP. Our results demonstrate the existence of overlap and distinct signaling pathways for which type of OFCs develops and suggest plausible elements responsible for phenotypic heterogeneity, revealing the complex genetic architecture of OFCs. Additionally, it will set up the foundation upon which would be possible for us to discover how the prior diagnostic panels are designed.

Wnt signaling pathway including wnt9a and irf6 has been reported to play key roles in craniofacial morphogenesis.[30,31] IRF6 and Notch ligand Jagged2 signaling were crucial for restricting palatal adhesion and fusion competence.[32] Craniofacial abnormalities may be caused by changes in transforming growth factor-beta (TGFβ) signaling.[33] TGFβ1 and TGFβ2 are believed to be primarily engaged in controlling the proliferation of the palatal mesenchyme whereas TGFβ3 has been suggested to have a significant impact on controlling the fate of midline epithelial cells during palatal fusion.[34] Perturbed hedgehog (HH) signaling particularly mutation in patched1 plays a major role in craniofacial development.[35] Based on the KEGG

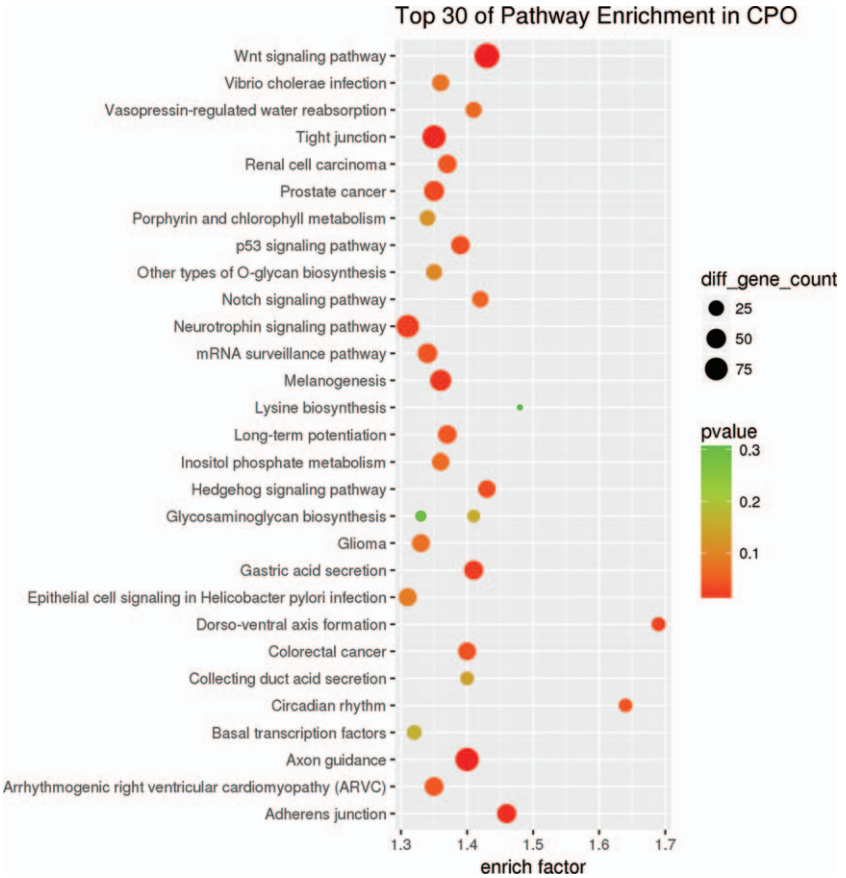

Figure 4. KEGG pathway analyses show the associated function of the target genes of the miRNAs dysregulated in CPO. Top 30 enriched pathways for the 9330 target genes of the 10 upregulated miRNAs and 3 downregulated miRNAs in CPO. Fisher's exact test is utilized to calculate the enrichment *P*-value. Based on the first letter of the path name, the terms/paths on the vertical axis are sorted in descending order. Enrichment factors are plotted on the horizontal axis, that is, the number of dysregulated genes/total number of dysregulated genes in the pathway/(number of genes in the pathway in the database/total number of genes in the database). The first 30 enrichment approaches are based on enrichment factors. Pathway in the number of genes ≥ 4, $P < .05$ is the selection criteria. *P*-values are expressed in different colors from green to red. The gene counts in the pathway are displayed by circles of various sizes. CPO = cleft palate only, KEGG = Kyoto Encyclopedia of Genes and Genomes, miRNAs = microRNAs.

pathway analysis, the predicted target genes of the upregulated and downregulated miRNAs in CLO, CPO, and CLP mainly participated in Wnt, Notch, TGF-beta, and Hedgehog signaling pathways, that is consistent with existing literatures.

Epigenetics is explained as genetic alterations in phenotype or gene expression that result from processes other than alterations in the basic DNA sequence. These processes contain, but are not restricted in, DNA methylation, microRNA impacts, and histone adjustments that change chromatin conformation. Recent studies suggest that different methylation profiles was found in distinct orofacial cleft (OFC) subtypes, representing a prospects with potential in discovering the possible impacts of epigenetic modifications on the aetiology of OFCs and/or as clinically functional biomarkers of OFC subtypes.[7]

Our study found that distinct plasma miRNAs were differentially expressed in different orofacial cleft (OFC) subtypes. Further analyzing the predictive target genes of nonoverlapping miRNAs in CLO, CPO, and CLP using KEGG pathway analysis, we found that the top 30 enriched enriched pathways were uniquely associated with CLO including nonhomologous end-joining, protein processing in endoplasmic reticulum, glycosphingolipid biosynthesis, valine, leucine and isoleucine biosynthesis, RNA polymerase, endocytosis, sulfur relay system, adipocytokine signaling pathway, protein export, and fatty acid biosynthesis. In contrast, 10 pathways of the top 30 enriched pathways were only linked with CPO, including colorectal cancer, vasopressin-regulated water reabsorption, porphyrin and chlorophyll metabolism, melanogenesis, arrhythmogenic right ventricular cardiomyopathy (ARVC), prostate cancer, renal cell carcinoma, basal transcription factors, lysine biosynthesis, and neurotrophin signaling pathway. Moreover, 10 pathways of the top 30 enriched pathways were only linked with CLP, including regulation of autophagy, caffeine metabolism, insulin signaling pathway, pancreatic cancer, bladder cancer, mTOR signaling pathway, lysine degradation, cyanoamino acid metabolism, hypertrophic cardiomyopathy (HCM), and dilated cardiomyopathy. Further elucidating the complex genetic architecture of OFCs may push us following the fundamental humanitarian aim of stopping orofacial clefts.

Taken together, we provide an integration analysis of these differentially expressed plasma miRNAs in subtypes of non-syndromic orofacial clefts. Distinct and overlapping signaling pathways were revealed to participate in the pathogenesis of CLO, CPO, and CLP. In the future, urgent need should be taken to examine the mechanism of potential target genes. This may provide new targets for future clinical prevention and treatment.

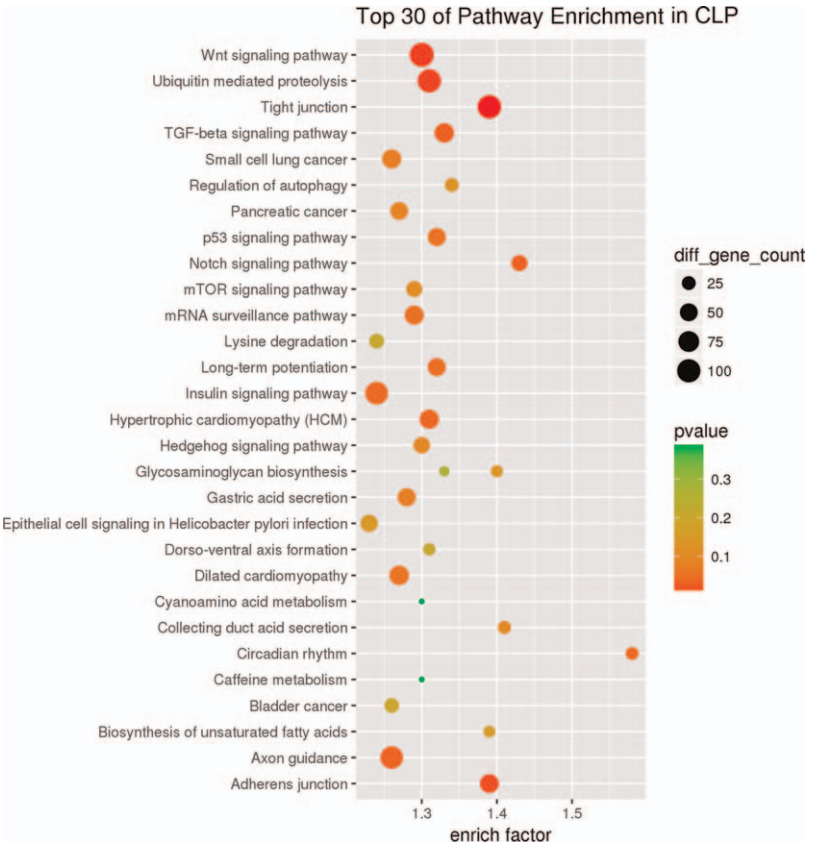

Figure 5. KEGG pathway analyses show the associated function of the target genes of the miRNAs dysregulated in CLP. Top 30 enriched pathways for the 11232 target genes of the 23 upregulated miRNAs and 6 downregulated miRNAs in CLP. Fisher's exact test is utilized to calculate the enrichment *P*-value. Based on the first letter of the path name, the terms/paths on the vertical axis are sorted in descending order. Enrichment factors are plotted on the horizontal axis, that is, the number of dysregulated genes/total number of dysregulated genes in the pathway/(number of genes in the pathway in the database/total number of genes in the database). The first 30 enrichment approaches are based on enrichment factors. Pathway in the number of genes ≥ 4, $P < .05$ is the selection criteria. *P*-values are expressed in different colors from green to red. The gene counts in the pathway are displayed by circles of various sizes. CLP = cleft lip with palate, KEGG = Kyoto Encyclopedia of Genes and Genomes, miRNAs = microRNAs.

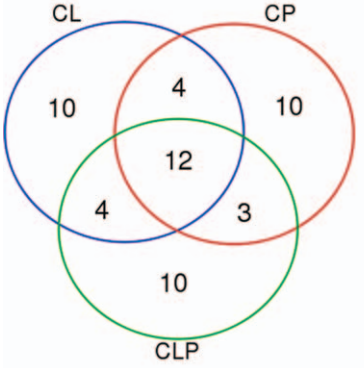

Names	total	elements
CL, CLP, CP	12	Long-term potentiation, mRNA surveillance pathway, Collecting duct acid secretion, Wnt signaling pathway, Glycosaminoglycan biosynthesis, Adherens junction, Epithelial cell signaling in Helicobacter pylori infection, Dorso-ventral axis formation, Tight junction, Notch signaling pathway, Hedgehog signaling pathway, Circadian rhythm
CL, CP	4	Inositol phosphate metabolism, Glioma, Other types of O-glycan biosynthesis, Vibrio cholerae infection
CL, CLP	4	TGF-beta signaling pathway, Biosynthesis of unsaturated fatty acids, Small cell lung cancer, Ubiquitin mediated proteolysis
CLP, CP	3	Axon guidance, p53 signaling pathway, Gastric acid secretion
CL	10	Non-homologous end-joining, Protein processing in endoplasmic reticulum, Glycosphingolipid biosynthesis, Valine, leucine and isoleucine biosynthesis, RNA polymerase, Endocytosis, Sulfur relay system, Adipocytokine signaling pathway, Protein export, Fatty acid biosynthesis
CP	10	Colorectal cancer, Vasopressin-regulated water reabsorption, Porphyrin and chlorophyll metabolism, Melanogenesis, Arrhythmogenic right ventricular cardiomyopathy (ARVC), Prostate cancer, Renal cell carcinoma, Basal transcription factors, Lysine biosynthesis, Neurotrophin signaling pathway
CLP	10	Regulation of autophagy, Caffeine metabolism, Insulin signaling pathway, Pancreatic cancer, Bladder cancer, mTOR signaling pathway, Lysine degradation, Cyanoamino acid metabolism, Hypertrophic cardiomyopathy (HCM), Dilated cardiomyopathy

Figure 6. Venn diagrams show the number of distinct and overlapping top 30 KEGG pathways among CLO, CPO, and CLP. The detailed distinct or overlapping KEGG pathways' information is listed at the right. CLO = cleft lip only, CLP = cleft lip with palate, CPO = cleft palate only, KEGG = Kyoto Encyclopedia of Genes and Genomes.

Author contributions

JZ and WS planned the experiment and conducted the data analyses. NW and JY performed the sample preparation and bioinformatics analyses. NW, JY, and TH performed the statistical analyses. NW and WS wrote and edited the manuscript.

Conceptualization: Weimin Shen.
Data curation: Tao Han, Weimin Shen.
Formal analysis: Tao Han.
Funding acquisition: Jijun Zou.
Investigation: Ni Wu.
Methodology: Ni Wu.
Project administration: Jun Yan.
Software: Jun Yan.
Supervision: Jijun Zou.
Validation: Jijun Zou.
Writing – original draft: Ni Wu.
Writing – review & editing: Weimin Shen.

References

[1] Rahimov F, Jugessur A, Murray JC. Genetics of nonsyndromic orofacial clefts. Cleft Palate Craniofac J 2012;49:73–91.
[2] Wang M, Yuan Y, Wang Z, et al. Prevalence of orofacial clefts among live births in China: a systematic review and meta-analysis. Birth Defects Res 2017;109:1011–9.
[3] Adeyemo WL, Butali A. Genetics and genomics etiology of non-syndromic orofacial clefts. Mol Genet Genomic Med 2017;5:3–7.
[4] Mossey PA, Little J, Steegers-Theunissen R, et al. Genetic interactions in nonsyndromic orofacial clefts in Europe-EUROCRAN study. Cleft Palate Craniofac J 2017;54:623–30.
[5] Yin X, Ma L, Li Y, et al. Genetic variants of 20q12 contributed to non-syndromic orofacial clefts susceptibility. Oral Dis 2017;23:50–4.
[6] Yu Y, Zuo X, He M, et al. Genome-wide analyses of non-syndromic cleft lip with palate identify 14 novel loci and genetic heterogeneity. Nat Commun 2017;8:14364.
[7] Sharp GC, Ho K, Davies A, et al. Distinct DNA methylation profiles in subtypes of orofacial cleft. Clin Epigenetics 2017;9:63.
[8] Dixon MJ, Marazita ML, Beaty TH, et al. Cleft lip and palate: understanding genetic and environmental influences. Nat Rev Genet 2011;12:167–78.
[9] Milger K, Gotschke J, Krause L, et al. Identification of a plasma miRNA biomarker signature for allergic asthma: a translational approach. Allergy 2017;72:1962–71.
[10] Schwarzenbach H, Nishida N, Calin GA, et al. Clinical relevance of circulating cell-free microRNAs in cancer. Nat Rev Clin Oncol 2014;11:145–56.
[11] Lo WY, Wang HJ, Chiu CW, et al. miR-27b-regulated TCTP as a novel plasma biomarker for oral cancer: from quantitative proteomics to post-transcriptional study. J Proteomics 2012;77:154–66.
[12] Deiuliis JA. MicroRNAs as regulators of metabolic disease: pathophysiologic significance and emerging role as biomarkers and therapeutics. Int J Obes (Lond) 2016;40:88–101.
[13] Zou J, Li J, Li J, et al. Expression profile of plasma microRNAs in nonsyndromic cleft lip and their clinical significance as biomarkers. Biomed Pharmacother 2016;82:459–66.
[14] Li J, Zou J, Li Q, et al. Assessment of differentially expressed plasma microRNAs in nonsyndromic cleft palate and nonsyndromic cleft lip with cleft palate. Oncotarget 2016;7:86266–79.
[15] Carlson JC, Standley J, Petrin A, et al. Identification of 16q21 as a modifier of nonsyndromic orofacial cleft phenotypes. Genet Epidemiol 2017;41:887–97.
[16] Ladd-Acosta C, Beaty TH. Integrating RNA expression identifies candidate gene for orofacial clefts. J Dent Res 2018;97:31–2.
[17] Balzano F, Deiana M, Dei Giudici S, et al. miRNA stability in frozen plasma samples. Molecules 2015;20:19030–40.
[18] Sivertsen A, Wilcox AJ, Skjaerven R, et al. Familial risk of oral clefts by morphological type and severity: population based cohort study of first degree relatives. BMJ 2008;336:432–4.
[19] Leslie EJ, Marazita ML. Genetics of cleft lip and cleft palate. Am J Med Genet C Semin Med Genet 2013;163C:246–58.
[20] Peng HH, Chang NC, Chen KT, et al. Nonsynonymous variants in MYH9 and ABCA4 are the most frequent risk loci associated with nonsyndromic orofacial cleft in Taiwanese population. BMC Med Genet 2016;17:59.
[21] Kondo S, Schutte BC, Richardson RJ, et al. Mutations in IRF6 cause Van der Woude and popliteal pterygium syndromes. Nat Genet 2002;32:285–9.
[22] Rahimov F, Marazita ML, Visel A, et al. Disruption of an AP-2alpha binding site in an IRF6 enhancer is associated with cleft lip. Nat Genet 2008;40:1341–7.
[23] Jugessur A, Shi M, Gjessing HK, et al. Fetal genetic risk of isolated cleft lip only versus isolated cleft lip and palate: a subphenotype analysis using two population-based studies of orofacial clefts in Scandinavia. Birth Defects Res A Clin Mol Teratol 2011;91:85–92.
[24] Kestler HA, Muller A, Gress TM, et al. Generalized Venn diagrams: a new method of visualizing complex genetic set relations. Bioinformatics 2005;21:1592–5.
[25] Sheehy NT, Cordes KR, White MP, et al. The neural crest-enriched microRNA miR-452 regulates epithelial-mesenchymal signaling in the first pharyngeal arch. Development 2010;137:4307–16.
[26] Wang J, Bai Y, Li H, et al. MicroRNA-17-92, a direct Ap-2alpha transcriptional target, modulates T-box factor activity in orofacial clefting. PLoS Genet 2013;9:e1003785.
[27] Warner DR, Mukhopadhyay P, Brock G, et al. MicroRNA expression profiling of the developing murine upper lip. Dev Growth Differ 2014;56:434–47.
[28] Ma L, Xu M, Li D, et al. A miRNA-binding-site SNP of MSX1 is associated with NSOC susceptibility. J Dent Res 2014;93:559–64.
[29] Xu M, Ma L, Lou S, et al. Genetic variants of microRNA processing genes and risk of non-syndromic orofacial clefts. Oral Dis 2018;24:422–8.
[30] Brown NL, Knott L, Halligan E, et al. Microarray analysis of murine palatogenesis: temporal expression of genes during normal palate development. Dev Growth Differ 2003;45:153–65.
[31] Dougherty M, Kamel G, Grimaldi M, et al. Distinct requirements for wnt9a and irf6 in extension and integration mechanisms during zebrafish palate morphogenesis. Development 2013;140:76–81.
[32] Richardson RJ, Dixon J, Jiang R, et al. Integration of IRF6 and Jagged2 signalling is essential for controlling palatal adhesion and fusion competence. Hum Mol Genet 2009;18:2632–42.
[33] Pelikan RC, Iwata J, Suzuki A, et al. Identification of candidate downstream targets of TGFbeta signaling during palate development by genome-wide transcript profiling. J Cell Biochem 2013;114:796–807.
[34] Meng L, Bian Z, Torensma R, et al. Biological mechanisms in palatogenesis and cleft palate. J Dent Res 2009;88:22–33.
[35] Metzis V, Courtney AD, Kerr MC, et al. Patched1 is required in neural crest cells for the prevention of orofacial clefts. Hum Mol Genet 2013;22:5026–35.